SunSailor: Solar Powered UAV

Faculty of Aerospace Engineering,
Technion IIT, Haifa, Israel,
Students' Project

A. Weider, H. Levy, I. Regev, L. Ankri, T. Goldenberg, Y. Ehrlich, A. Vladimirsky, Z. Yosef, M. Cohen.
Supervisor: Mr. S. Tsach, IAI

ABSTRACT
This paper summarizes the final project of undergraduate students team at the Faculty of Aerospace Engineering at the Technion IIT, Haifa, Israel. The team was formed to design, build, test and fly a Solar Powered Unmanned Aerial Vehicle with the final goal of breaking the world record for distance flight under certain limitations. Until this moment two UAVs were built at the Technion Workshop. The first flew its first solar flight on June 29th 2006. It crashed on its third solar flight. The second was built in 54 days, flew and crashed on its maiden solar flight. The third UAV is under construction.

1 Introduction

The FAI (The World Airsports Federation) world record for the F5-SOL Category today was set on June 13, 1997 and is 48.21 Km. Our goal was to set a new record at 139 Km. The whole flight must be radio controlled and no autopilots of any kind may be used to fly or help flying the UAV. The route for the record setting flight was decided to be over the Arava highway, Israel, from Hatzeva to Eilot. Global Radiation Analysis for the flight route showed best conditions from June to August.
Other main objectives of the project were proving the feasibility of Solar Powered, Low Altitude Long Endurance UAVs at certain design limitations and advancing the use of clean power sources in subsonic aviation. Aside from potential military applications, civil demands for Long Endurance UAVs are growing daily. These will be able to replace communication, scientific and environmental satellites in the future, suggesting a cost effective replacement to satellites technology. They will be able to monitor large crops, forests and wildlife migration. The Solar Powered UAVs use an unlimited power source for propulsion and other electrical systems. Using Photovoltaic (PV) cells, solar radiation is converted into electric power and then converted into kinetic energy by the electric motor. The main difficulty as for today is the low efficiency of both PV cells and motors. This paper presents the development of the Sunsailor, a Solar Powered UAV, discussing the following issues:

- Project objectives and requirements.
- UAV's design.
- Manufacturing and Ground Tests.
- Solar Array design and tests
- Flight Tests

Figure 1: Sunsailor2 Solar flight

2 Project Objectives

The project has a number of objectives:

1. Enabling the students to integrate the knowledge acquired in their academic studies and experiencing an air vehicle development, manufacturing and testing process.
2. Introducing the students airborne systems and technologies not included or briefly mentioned in the undergraduate academic studies (PV cells, autopilot, electric motors, etc.)
3. Setting a new world record for lightweight Solar Powered UAV.
4. Advancing clean power sources for aviation purposes in particular.

3 Design Requirements

3.1 Aircraft Requirements

- Electrical motor propulsion.
- Radio controlled flight without the help on any telemetry.
- Maximum upper surfaces area of $1.5m^2$.
- Maximum Weight of 5 Kg.
- Only Solar Cells are permitted as the propulsion system power source.

3.2 Flight Plan

- The Sunsailor UAV will be hand-launched and take off from Hatzeva Junction, a few kilometers south of the dead sea, Israel. Most of the flight path is 50-100 meters west of the Highway. At some points the path will cross the highway to the east to avoid any near cliffs.
- General heading is south in order to fly downwind.
- Belly landing will be performed on a soft surface near Eilot, a few kilometers north of Eilat.
- The UAV will be escorted by a vehicle carrying 3 pilots and a designated driver. Therefore ground speed must be at least 50kph as the law requires such minimum speed along this highway.
- Flight Altitude will not exceed 500ft above ground level and therefore will not interfere with civil aviation although the flight path is just under the low civil routes in the area.
- Traffic Police and Air Force control will be notified about the flight.

Figure 2: Flight Plan for record setting. 139Km.

4 Work Organization and Timeline

4.1 Team Architecture

As the project involved many aspects of design and manufacturing each of the students was given several different fields in design and all worked on manufacturing once design and acquisition were done.4 Pilots were chosen by reputation and flying experience with electric sailplanes. The design aspects were geometry, aerodynamics and stability, structure, landing and takeoff concepts, performance, subsystems, solar array design, propulsion and design for manufacturing. A project manager was selected to integrate the different fields and supervise acquisition and manufacturing. His responsibility was to organize work, set the time frame and priorities. An IAI advisor directed the group to achieve each milestone in the most efficient way, while assimilating the industry's project conducting methods.

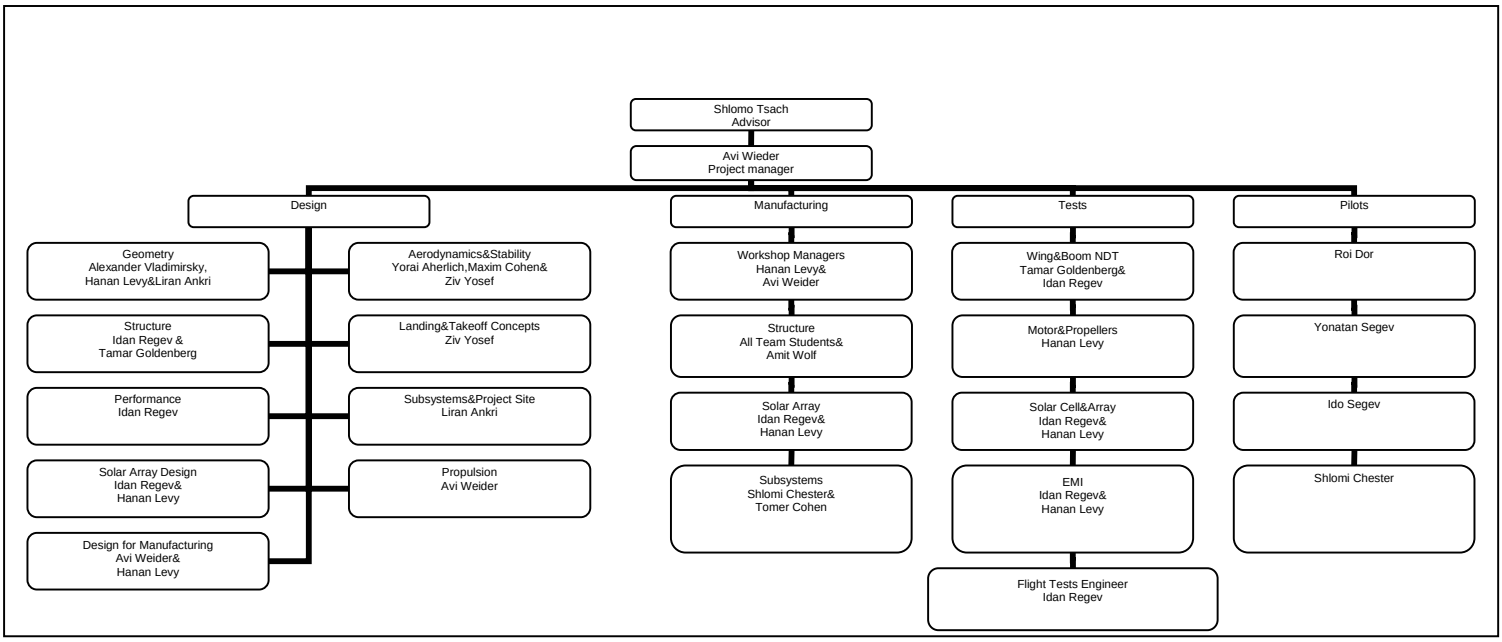

Figure 3: Team Architecture

4.2 Schedule

Design was concluded after two full semesters. First semester was dedicated to preliminary design and was concluded in a Preliminary Design Review (PDR). In the second semester a comprehensive design for manufacturing was completed and manufacturing began. The semester work was concluded in a Critical Design Review (CDR). During the weekly meeting the team reviewed each field's progress and decided the next assignments. The project manager set priorities and summarized the meeting conclusions. As acquisition and cutting of the solar cells took a very long time, first solar flight was delayed by one month.

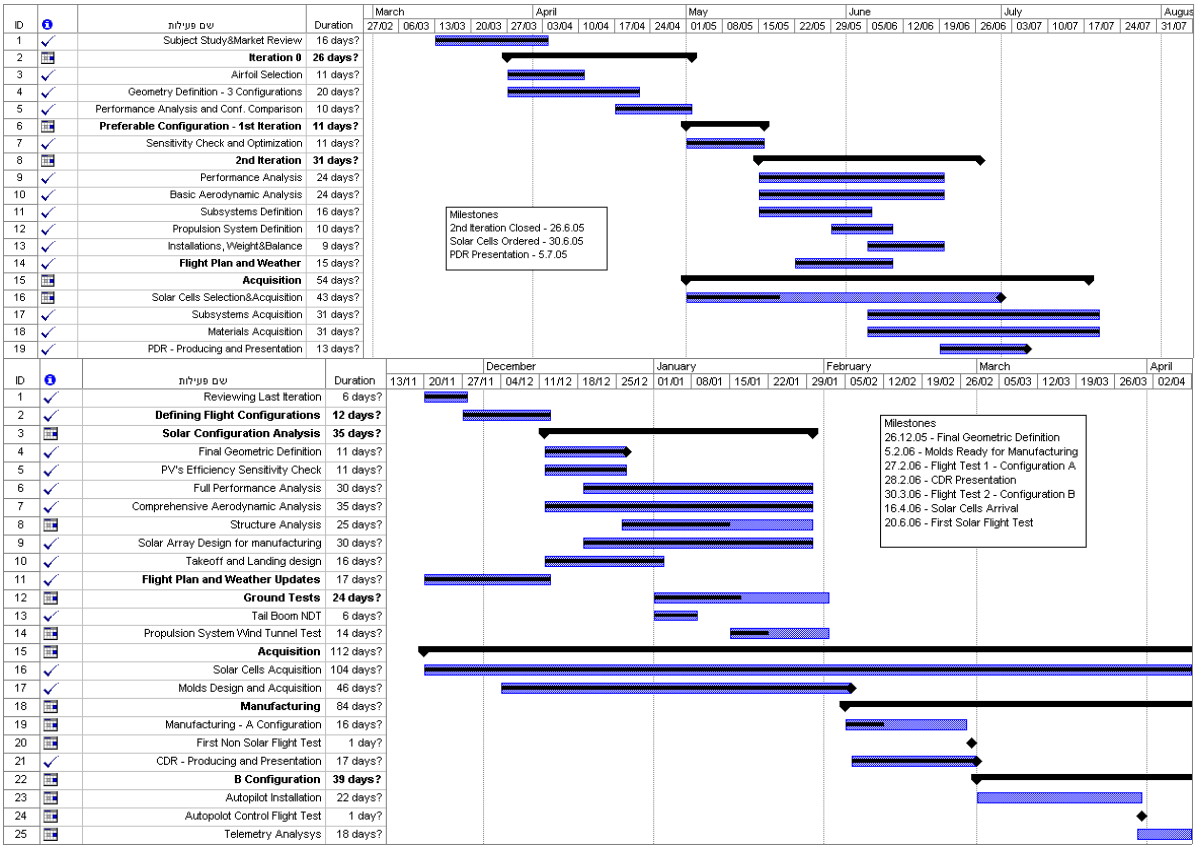

Figure 4 : Semester 1&2 Gant Charts.

5 Air Vehicle Description

5.1 Conceptual Design

As Efficiency of commercial solar cells is still very low, the platform must be some sort of a sailplane with high Aspect Ratio (AR) and high lift over Drag (L/D). Three configurations were examined, a conventional sailplane, flying wing and a twin boom configuration. After evaluating the advantages and disadvantages of each configuration, the conventional approach was chosen due to lower Drag (D) and higher cruise velocity. Also this approach is well known for both theory and manufacturing, thus minimizing the risks, times and costs.

After deciding on the conventional configuration the team checked performance for double vs. single motor, conventional tail vs. “V” shaped tail, low AR vs. high AR and small vs. large ailerons.

Different takeoff and landing concepts were also examined. The team chose the hand-launched takeoff and belly landing. This way there is no need for gear or the excess weight of any other landing device.

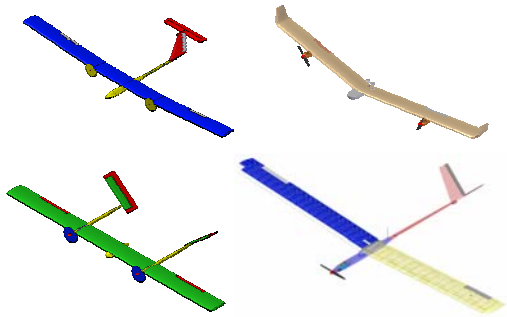

Figure 5: Three configurations and the final Sunsailor concept.

5.2 Aircraft's Definition (for Sunsailor1)

Max T.O Weight:	3.6[Kg]
Length:	2.2[m]
Wing Airfoil:	SD7032
Span:	4.2[m]
Wing Area:	1.35[m^2]
Aspect Ratio:	13.15
Wing Dihedral:	3.5°
Tail Airfoil:	NACA0007
Horizontal Tail AR:	5.77
Tail Aperture:	90°

Power Plant

Electric Motor:	Hacker B50-13S
Speed Controller:	Hacker X-30
Gear Ratio:	6.7:1
Propeller:	15"X10"

Solar Array (Sunsailor1/Sunsailor2)

PV's Area:	0.943/1.097[m^2]
PV's Efficiency:	21%
PV's Weight:	0.66/0.77[Kg]
PV's Maximum Power:	100/140[W]

5.3 Aircraft's Geometry

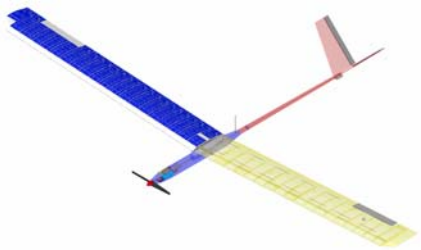

Figure 6: Sunsailor Isometric View

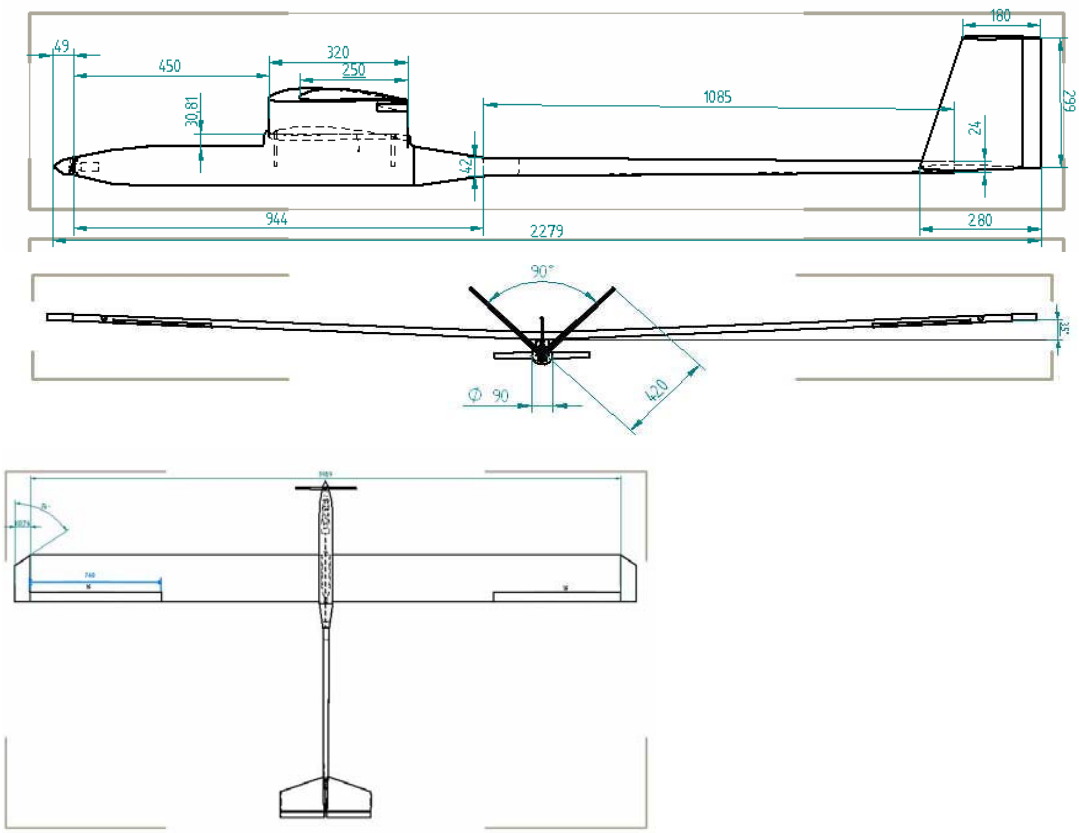

Figure 7: Sunsailor Geometry

5.4 Characteristic Parameters

$\frac{b}{\sqrt{S_{wet}}} = 2.18$	$C_{fe} = 0.0030$
$\left(\frac{T}{W}\right)_{takeoff} = 0.3$	$C_{D_0} = 170[counts]$
$\frac{W}{S_{wing}} = 2.66\left[\frac{Kgf}{m^2}\right]$	$\left(\frac{L}{D}\right)_{\max} = 20.23$

Table 1: Sunsailor's Characteristic Parameters

5.5 Performance

The basic flying qualities could be tested during flight using telemetry data and are presented here for both design and tested values:

Quality Designed/Tested
Stall Airspeed: 12/13 [knots]
Max. Airspeed: 33/38 [knots]
Cruise Airspeed: 25/23 [knots]
Max. Climb Rate: 300/240 [ft/min]
Solar Array Power
Required for takeoff: 50/70 [Watt]
Wing Max. Load Factor: 2.8/4

5.6 Weight & C.G Estimation Vs. Reality

Weight and C.G estimation was made during design. While systems weight could easily be decided structure and wiring were estimated using several assumptions. Estimated weight was 3.818 [Kg] and estimated C.G at 34.93% chord. The true weight was smaller only by 200 [gr] and C.G was more forward by less than 3%. Therefore the former estimations were relatively accurate.

Sunsailor1 Weight Breakdown				
Moment [gr X m]	Arm [mm] from Firewall	Weight [gr]	Component	
762.34	543.32	1403.1	Wing	Structure
117.30	509.18	230.3	Fuselage	
101.60	1270.00	80	Tail Boom	
159.84	2070.41	77.2	Tail Servos	
42.70	610.00	70	Ailerons Servos	Avionics & Subsystems
84.40	2110.00	40	Tail Servos	
164.70	610.00	270	Autopilot&Com.+Ant.	
92.00	255.56	360	Systems Battery	
4.90	20.00	245	Electric Motor	Propulsion
1.90	50.00	38	Speed Controller	
0.30	15.00	20	Prop+Spinner	
410.52	622.00	660	PV cells	Power Supply
45.00	450.00	100	Wiring	
1987.50	Total Moment [Kg X m]	3593.6	Total Weight [gr]	
From motor Firewall	553.05	mm	Xcg	
From L.E	32.20	%chord		
From L.E	46.20	%chord	Xn	
	14.00	%chord	Stability Gap	

Table 2: Sunsailor1 Weight Breakdown

6 Aerodynamic Design

As the main goal of the project was to set a distance flight record using solar radiation as the energy source a priority was given for high velocity at low Reynolds numbers with minimum power requirements. This resulted in the chosen airfoil and Aspect Ratio. On the other hand compromises were made for longitudinal and lateral stability and control as the platform is not intended for any sharp, sudden maneuvers. As upper surfaces are constrained both stabilizers and tail control surfaces are smaller than expected and leave very small margins for lateral stability and control. The use of a V-Tail is a result of the areas and balance constraints. The final configuration was analyzed using

Vortex Lattice Method (VLM) due to the lack of formulas regarding V-tail.

6.1 Properties of the chosen airfoil, SD7032, and changes due to solar array mounting

The Selig-Donovan 7032 airfoil is very thin, thus allows high velocity with smaller drag than wider airfoils. It is designed for low Reynolds numbers sailplanes as it produces high lift at low drag. The solar array mounted on the upper camber breaks the camber smoothness. As the array starts 14.25% from the Leading Edge (L.E) and completes the upper camber in 8 ribs it has very little effect on the flow. Moreover, the roughness of the new camber assures a turbulent flow over the wing. The new airfoil was called SD7032_P for reference.

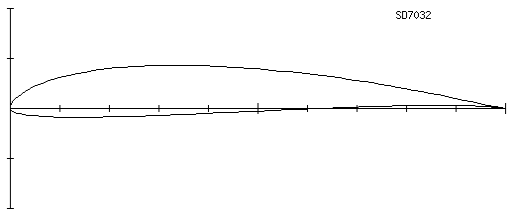

Figure 8: SD7032 Airfoil

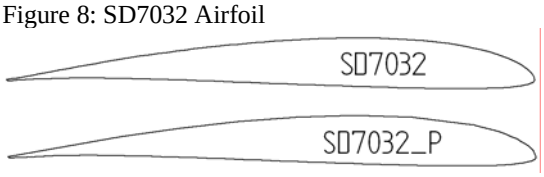

Figure 9: SD7032 Vs. SD7032_P, a difference can hardly be noticed.

$C_{l_{\max}} = 1.35$	$C_{l_\alpha} = 5.72$
$\left(\frac{C_l}{C_d}\right)_{\max} = 83$	$\frac{t_{\max}}{c} = 9.97$
$C_{m_0} = -0.085$	$\alpha_{0_L} = -4.61^\circ$

Table 3: SD7032 Airfoil's Characteristics

6.2 Parasite Drag Analysis

Parasite drag was calculated using empirical formulas taken mainly from Ref. 1. Turbulent flow was assumed for the fuselage and wing (SD7032_P roughness) and Laminar flow over the tail. The calculated parasite drag values for these are presented below. The V-tail produces smaller parasite drag than conventional tail.

Component	Reynolds Number at cruise	C_{D_0}
Fuselage	2,112,000	0.0014
Wing	335,000	0.0087
Tail	246,000	0.0012
Total C_{D_0}	0.0170	
$\frac{S_{wet}}{S_{ref}}$	5.57	
C_{fe}	0.0030	

Table 4: Parasite Drag Breakdown

6.3 Lift, Drag and Moment Characteristics

Aircraft's AR is 13.15. This is rather low for gliders/sailplanes but the wing dimension had to take the solar array and constraints into account. Yet, the aircraft's aerodynamic efficiency and L/D ratio are high enough. The addition of winglets was considered. However, large enough winglets to be effective might block the sunlight to the tip PV cells, thus causing a drastic drop in power. Therefore, no winglets were used. Using the airfoil polar and simple calculations from Ref. 1, Lift, Drag and Moment coefficients for the Sunsailor 3D wing can be seen in the following figures. Max L/D as can be seen is 20.23.

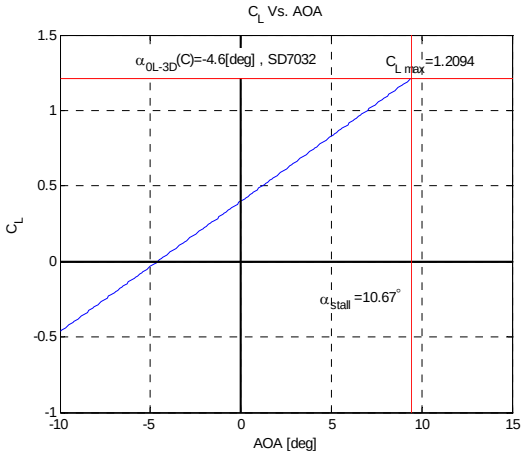

Figure 10: Lift Coefficient Vs. Angle of Attack (AOA).

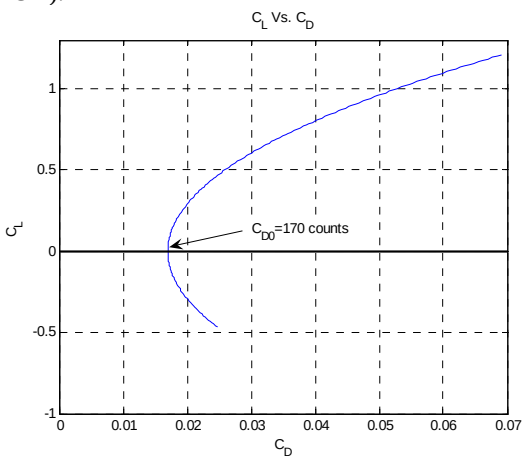

Figure 11: Lift Coefficient Vs. Drag Coefficient.

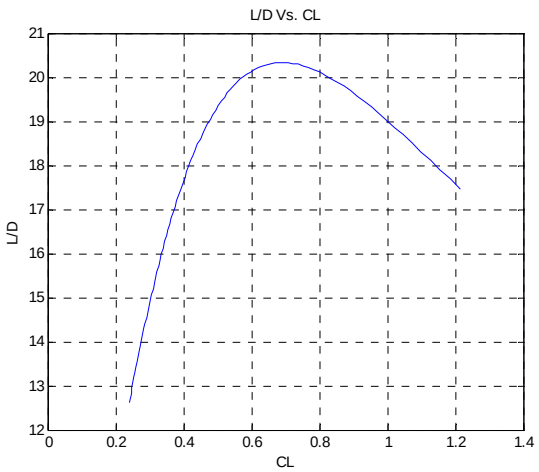

Figure 12 : L/D Vs. Lift Coefficient.

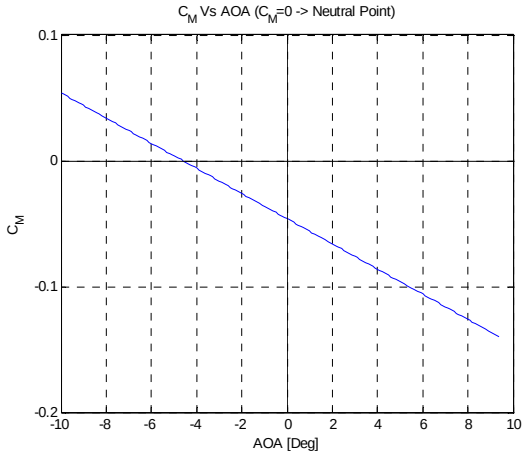

Figure 13: Moment Coefficient Vs. AOA.

6.4 Longitudinal Stability

In order to determine the static longitudinal stability properties of the aircraft C.G and Neutral Point (X_n) positions were calculated. These values can be found in table 2. The stability gap (or margin) is $\left(X_{C.G} - X_n\right)/C_{mac} = 14\%$ which means a very stable longitudinal behavior. The use of a conventional tail with the same aspect ratios and tail volume would mean larger tail weight. Due to the tail's long arm, any additional weight would critically change C.G position moving it closer to the neutral point and radically decreasing longitudinal stability. Therefore Horizontal Tail volume is smaller than what would be expected, but sufficient for moment balancing. The neutral point was calculated using Etkin's and verified using VLM code called AVL (Ref. 2,4).

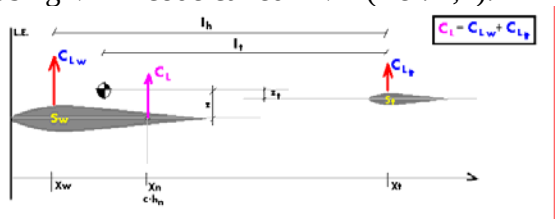

Figure 14: Neutral Point Position

6.5 Trim Analysis

As no flaps are used, trim analysis is quite simple. A calculation was made for conventional tail and then properly adjusted to the V-tail controls position. It was found that 30 degrees deflection of the elevator-rudder (both sides of the V-tail are deflected in the same direction) will give all the required C_L values.

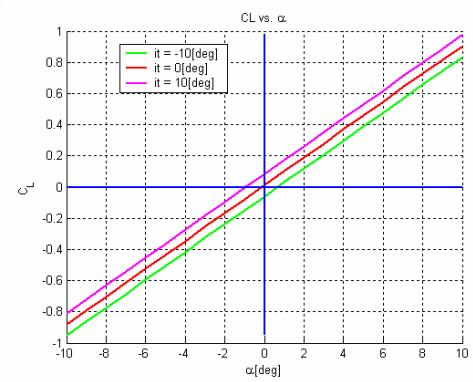

Figure 15: C_L Vs. AOA Trim Analysis for Elevators deflections

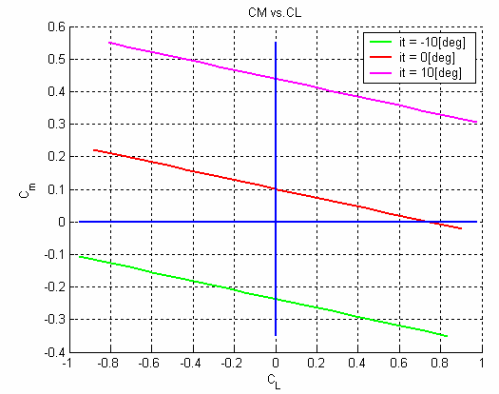

Figure 16: C_m Vs. C_L Trim Analysis for Elevator Deflections

Longitudinal dynamic stability was analyzed using AVL and compared to empiric calculations. Pitch rate was checked with and without slide angle for both takeoff and cruise. All figures show sufficient stability and maneuvering capabilities even in moderate side wind.

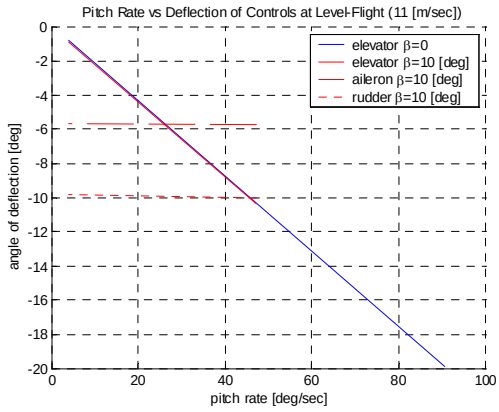

Figure 17: Elevator Deflection Vs. Pitch Rate at Cruise.

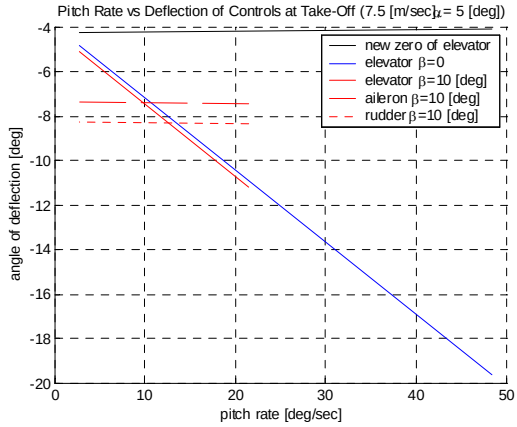

Figure 18: Elevator Deflection Vs. Pitch Rate at Takeoff.

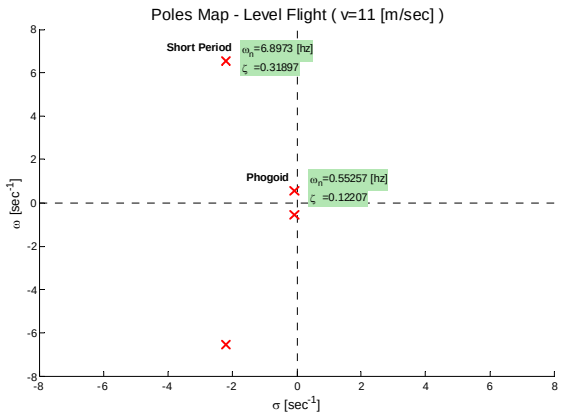

Figure 19: Longitudinal Dynamics.

6.6 Lateral Stability Analysis

Due to surfaces constraint and the tail weight critical influence on C.G., Rudder surfaces are smaller than expected. This results in a very small

Vertical Tail volume. Along with the a constraint on wing dihedral, due to sunlight-PV cells angle, lateral stability analysis shows a minor instability in the spiral mode. As all known solutions were constrained and thus rejected, it was decided that the instability is reasonable and will only cause small annoyance to the pilots during turns. All Lateral Stability was analyzed using AVL and compared to empiric calculations where possible.

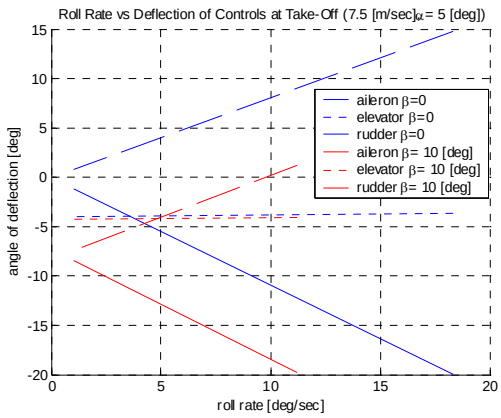

Figure 20: Controls' Deflections Vs. Roll Rate at Takeoff.

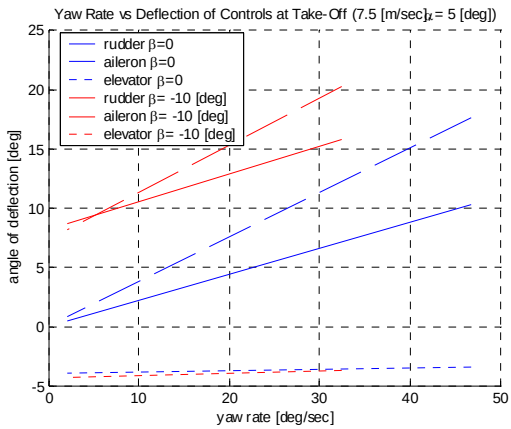

Figure 21: Controls' Deflections Vs. Yaw Rate at Takeoff.

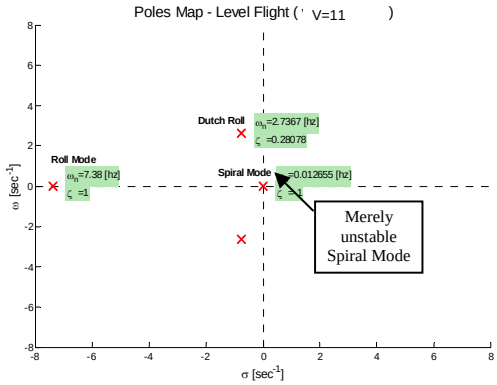

Figure 22: Lateral Dynamics.

6.7 Aerodynamic Coefficients Via VLM Analysis

The VLM code used for the aerodynamic analysis is called AVL (Ref. 3). The code receives inputs for the vehicle geometry, 2D Lift & Drag polar and Weights & Moments of Inertia Breakdown. Output can be received for coefficients, pressure and forces distribution, C.G and neutral point position and dynamic behavior at different flight conditions. The VLM – Vortex Lattice Method Divides wing and tail surfaces to a user-defined number of panels (lattices) both chord wise and span wise. Each panel contains a horseshoe vortex. Border and Control conditions are set and the induced speed is calculated at each point by forcing a zero perpendicular speed constraint. Using the resulted velocities, calculation of aerodynamic capabilities is simply done.

Stability and Control Derivatives:

Longitudinal Coefficients		Lateral Coefficients	
$C_{l\alpha}$	5.47[1/rad]	$C_{Y\beta}$	-0.19 [1/rad]
$C_{M\alpha}$	-0.6[1/rad]	C_{Yp}	-0.13 [s/rad]
C_{Mq}	-0.134 [s/rad]	C_{Yr}	0.14 [s/rad]
Controls		$C_{L\beta}$	-0.11 [1/rad]
$C_{L\delta e}$	0.003[1/rad]	C_{Lp}	-0.7[sec/rad]
$C_{L\delta a}$	-0.003[1/rad]	C_{Lr}	0.11[sec/rad]
$C_{L\delta r}$	-0.00015 [1/rad]	$C_{N\beta}$	0.047[1/rad]
$C_{Y\delta a}$	-0.0006[1/rad]	C_{Np}	-0.03[sec/rad]
$C_{Y\delta r}$	-0.002[1/rad]	C_{Nr}	-0.04[sec/rad]
$C_{M\delta e}$	-0.015[1/rad]		
$C_{N\delta a}$	0.0001[1/rad]		
$C_{N\delta r}$	0.0008[1/rad]		

Table 4: Non-Dimensional Stability & Control Derivatives.

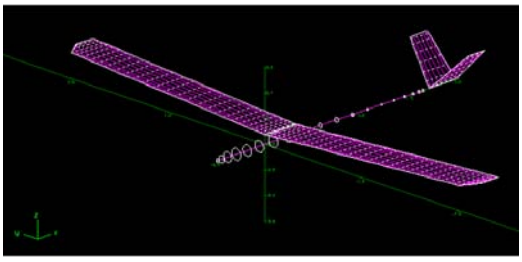

Figure 23: Sunsailor Geometry input to AVL

7 Structural Design

The large **Wing** span means aero-elasticity influences on aerodynamics and especially on dynamic stability and control. In order to minimize such interferences and movements in the solar array, the wing should have been designed to be rigid as possible.

However tradeoffs with wing weight results in a slightly elastic wing.
Two concepts were examined for the wing structure:

- A fully closed wing. Full bi-axial Kevlar skin set 45 degrees span-wise from L.E to T.E with a strengthened forward D-box and beam, all produced in MDF molds, with few inner ribs from Balsa (cut with laser CNC).
- A Forward Glass-Balsa-Carbon D-Box and beam, produced in molds with large number of Balsa ribs to hold a thin stretched Nylon (Solite) cover.

The second concept was chosen, applying less weight and an easy access to the Solar Array wiring (that proved very useful in later flight tests).
A step was designed in the D-Box and ribs to accommodate the Solar Array when ready without protruding from the original airfoil geometry.

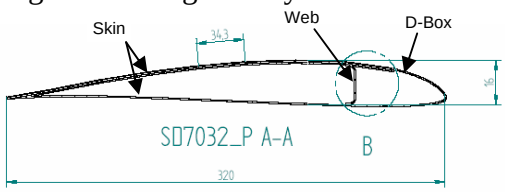

Figure 24: Wing Skin & D-Box Structure.

Forward "U" Beam was also manufactured in MDF mold. A Carbon-Balsa-Carbon laminate was used, where one bi-axial carbon layer was set at 45 degrees and the other on 0/90 degrees. Balsa fibers were set perpendicular to the span. Beam Flanges were made of 3 unidirectional carbon layers to assure reduce elasticity and enlarge strength under bending.

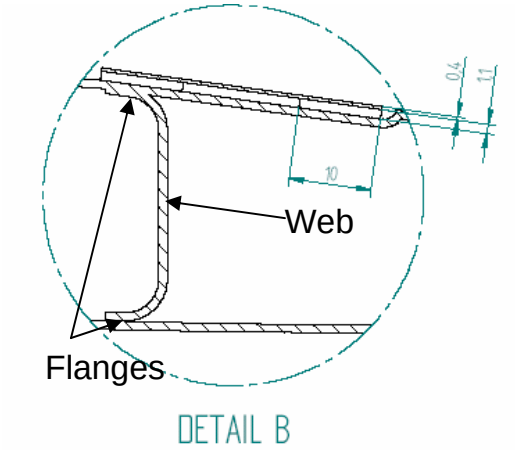

Figure 25: Forward Beam Structure.

Fuselage was manufactured in two molds, upper and lower. A Carbon-Balsa-Carbon laminate gave sufficient strength for belly landings. The bi-axial layers were set at 45 and 0/90 degrees to X axis (opposite to body heading through body centerline). The wing mounting extension was strengthened with two more carbon layers and unidirectional carbon stringers.

Figure 26: Sunsailor Fuselage.

Tail Boom was manufactured by a sub-contractor, using Carbon-Balsa-Carbon/Kevlar laminate.
Tail was manufactured from Balsa, applying forward and backward beams, ribs, stringers and a thin silver mylar skin.

Figure 27: Sunsailor Tail & Tail Boom

Main considerations taken for structural design were:
Weight and Strength – High Strength to weight ratio was mandatory to allow low weight for considerably large wing and the belly landing requirement. The use of composite materials, lightweight balsa, molds and drying under vacuum resulted in a high ratio as requested.
Solar Array Mounting and Access – An easy access to both sides of the solar array must be possible for maintenance and repairs. Therefore either a penetrable and replaceable cover is required as skin, or a mechanism that allows the removal of parts of the solar array. The Solite skin can easily be cut where needed and later patched with very small extra weight.
Construction Simplicity and Cost Effective – MDF molds were ordered from a sub-contractor for wing and fuselage and allowed very simple and high quality manufacture of these components. The MDF mold price is about one third that of an aluminum mold. Tail Boom which is complicated to manufacture was ordered from a sub-contractor for two parallel projects. This large order lowered the booms price by 25%.

7.1 V-n Diagram

A V-n diagram was plotted using the linear FAR 23.333 model for gusts amplitude. An adjustment to this model was made using a Statistical Dynamic model fitted to the wing load, lift coefficient and cruise speed of the Sunsailor. Vertical Gusts average speed taken was 10 feet per second that was calculated using these models and the average gust velocity in the record flight area. It can be seen in the next figure that the Maximum Positive Load factor is 3g.

Negative Load Factor is -1g. These values are acceptable considering the aircraft was never designed for any sharp maneuvering or strong gusts.

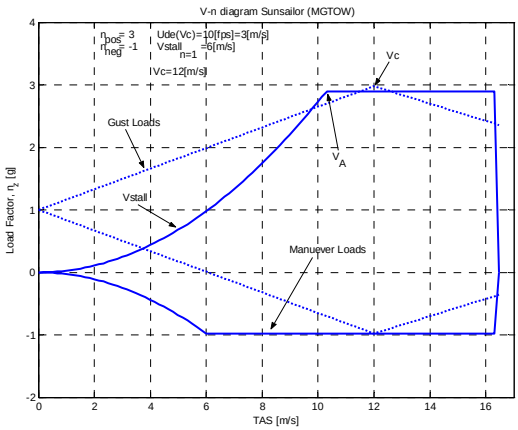

Figure 24: V-n Diagram

Forces and Moments were calculated for highest velocity and load factor.

7.2 Forces and Moments Distribution

Forces and Moments distribution were calculated for a 3g load factor at 16[m/s]. The lift, drag and pitch moment distributions were calculated using the Shrenk approximation. This approximation "fixes" the elliptic distribution by averaging it with a constant one. The calculations were made at 41 stations along the semi-span with higher density at the wing tip. It can be seen that the maximum loads are applied at the root and zeros at the wing tip.

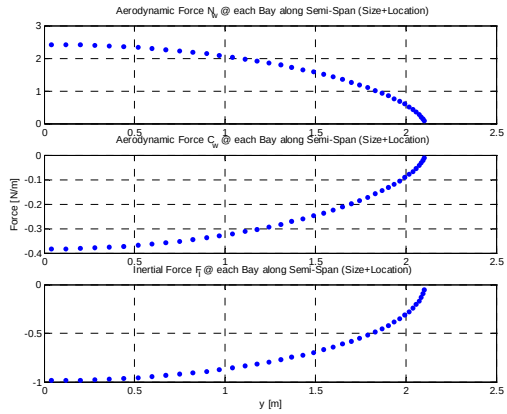

Figure 25: Aerodynamic and Inertial Forces Distribution along the semi-span.

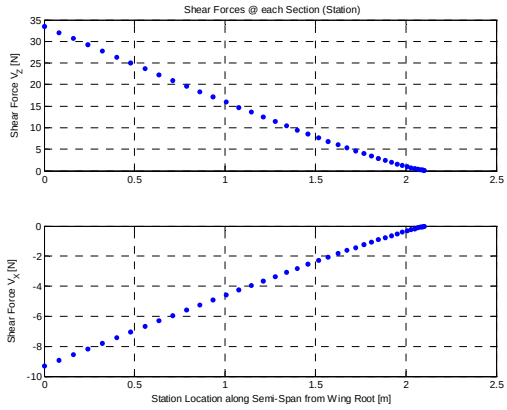

Figure 26: Shear Forces Distribution along the semi-span.

Compression and Tension stresses were calculated along the beam on both upper and lower flanges and compared to Euler Buckling loads to check for the ribs distribution validity. Using a safety factor of 1.2 the stresses are still lower than the Euler stresses and therefore the beam and ribs design should not buckle under tension.

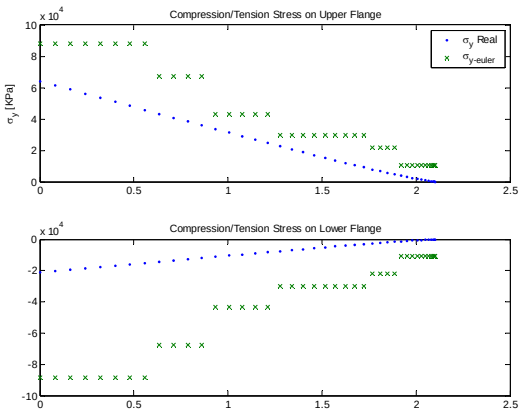

Figure 27: Calculated Tension Stress along the flanges Vs. Euler Buckling Stress.

8 Vehicle's Systems

8.1 Propulsion

The use of two motors was considered to allow redundancy. However, one larger motor means less weight and larger propeller, which has a higher efficiency. Moreover, the electric and control systems for 1 motor are much simpler. As a result, 1 motor configuration was selected. Landing Belly also constrained us to folding propellers to avoid the propeller hitting the ground when landing.

8.1.1 Thrust and Power requirements

Using the aerodynamic calculations and assuming a 4 [Kg] vehicle weight required thrust and power were calculated and than translated to Motor Input Required Power using motor, gearbox and propeller efficiencies. Minimum required power for cruise is 40[W] at 7.5[m/s]. Maximum cruise velocity requires 70[W]. Global Radiation data and solar array efficiency show a minimum produced power of 80[W] at the planned time and place for the record flight.

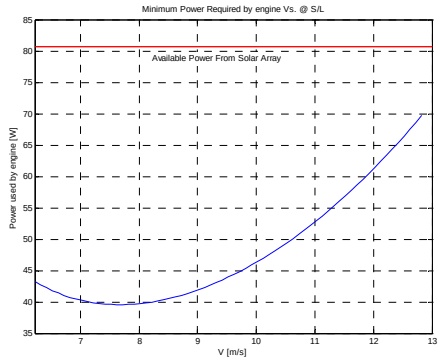

Figure 28: Required Motor Power Vs. Velocity at Cruise.

8.1.2 Motor and Propeller Properties

Motor Properties

The chosen motor, Hacker B50-13S with 6.7:1 Gearbox is a brushless electric motor and has the following properties:

Motor Constant K_v [RPM/V]	2800
No Load Current I_0 [A]	1.7
Resistance [Ω]	0.0153
Max. Continuous Current [A]	35
Max. Peak Current [A]	55
Max. LiPo Cells in Serial	5
Max Continuous Power [W]	650

Table 5: Hacker B50-13S Electric Properties

Motor Weight [gr]	200
Gearbox Weight [gr]	45
P.G shaft diameter [mm]	6
Shaft Length [mm]	16

Table 6: Hacker B50-13S Physical Properties

Electric Speed Controller (ESC)

Brushless motors require speed controllers. The chosen speed controller Hacker X-30 was chosen for its light weight and under the assumption that the solar array current will not be more than 15A under any circumstances. The X-30 also provides a Battery Eliminator Circuit (BEC) that allows the use of solar array power entering the controller for servos operation as well as motor

operation. However, when heating up the controller electronics might seize to function and perform a reset. The reset eliminates all servo and motor activity and requires an idle throttle command to renew operation.

Controller Weight [gr]	24
Max. Continuous Current [A]	30
Max. Peak Current [A]	35
BEC servos	2-4
Cutoff Temperature [°C]	110
Max. LiPo cells in serial	3

Table 7: Hacker X-30 Properties

Propeller Properties

The chosen propeller, a folder AeroNaut CAM, was selected using an electric propulsion system performance testing software, MotoCalc. After deciding on the belly landing concept a folding propeller was mandatory. Propeller diameters and pitches were checked for the required thrust at takeoff and cruise and for the motor RPM. The max propeller speed is 4700 (for 11.1V motor voltage). The chosen propeller has a 15" diameter and 10" pitch. This allows enough thrust at takeoff with full throttle and at the required cruise speed at 70% throttle with 65% propeller efficiency and 50% controller-motor-propeller system efficiency. .

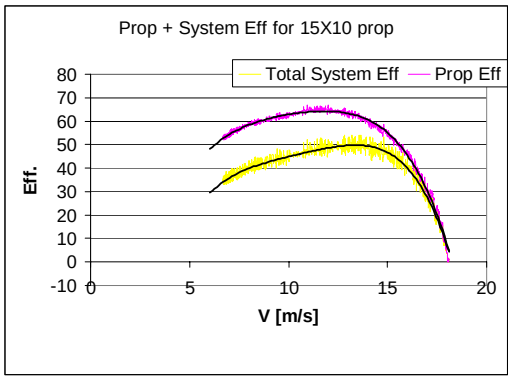

Figure 29: 15"X10" Propeller & Propulsion System Efficiency Vs. Flight Velocity.

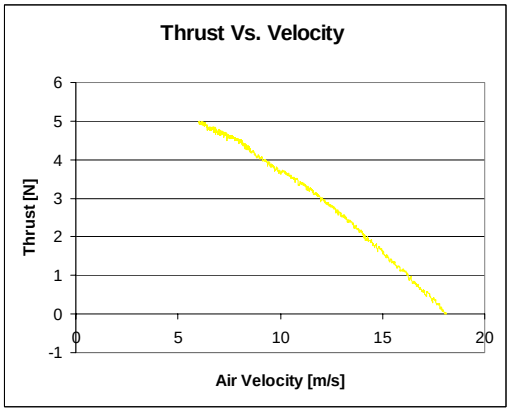

Figure 30: 15"X10" Propeller. Thrust Vs. Velocity (Full Throttle).

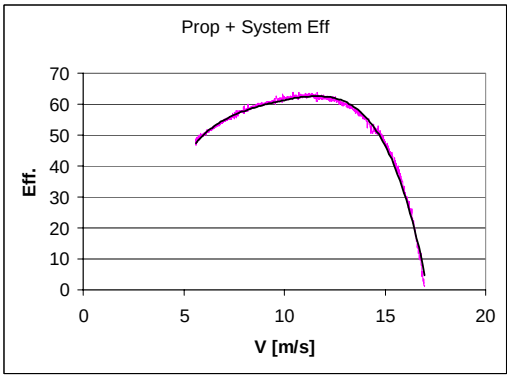

Figure 31: 14"X9" Propeller Efficiency Vs. Flight Velocity.

All the above figures were extracted from wind tunnel test data, without corrections for wall interferences and in order to choose the best propeller for cruise.

8.2 Avionics

Servos chosen were lightweight and produced enough torque for aileron and rudder-elevator. The brand was replaced for the second Sunsailor to increase reliability, trading off with a small extra weight.

Aileron Servo HS-125MG	
Weight [gr]	24
Torque [Kg X cm]	3.0
Rudder-Elevator Servo HS-65MG	

Weight [gr]	12.6
Torque [Kg X cm]	1.8

Table 8: Servos Properties

Autopilot was used for telemetry downloading and as a backup system for radio control loss. A switch was installed in the radio controller that allows a voluntary transfer between user and auto control. The autopilot, always monitoring radio control incoming commands and downloading telemetry, can identify loss of communication with the radio controller and automatically takes control over the flight after a number of seconds. If this should happen, the ground station computer would alert its operator. Telemetry can be seen on the ground station computer and consists mainly of incoming commands, rates, accelerations, position (via GPS), velocity (via barometric reading) and number of different flight status indications and warnings. The autopilot can also navigate the aircraft to an exact location or from-to two determined points on the map.
The autopilot itself without the telemetry communication card and antennas weight only 28 grams and was ideal for the aircraft.

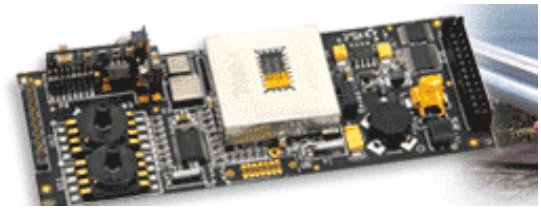

Figure 32: The Autopilot Card including all gyros and GPS receiver.

UHF Receiver and amplifier were used to ensure larger than normal radio control range to allow greater liberty for the pilots along the flight route.

8.3 Systems Installations

Motor, propeller and spinner were installed at the forward end of the fuselage. Telemetry and Radio Control Antennas were installed on upper half of the fuselage ahead of the wing. GPS antenna was installed on the upper half behind the wing. Autopilot system was installed in the fuselage under the wing as close as possible to aircraft's C.G.

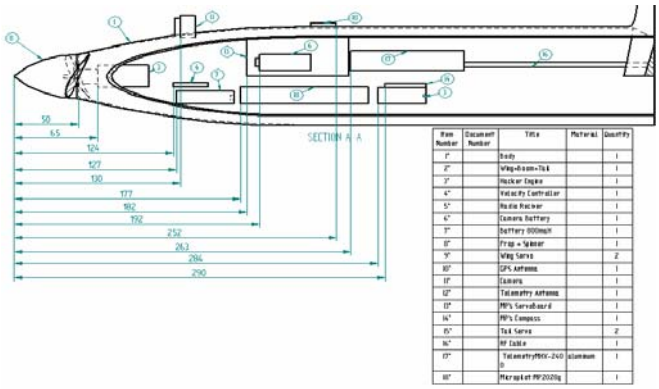

Figure 33: Systems Installations Design for Sunsailor1

Component	Arm from Wing L.E. [m]
Hacker B50 13S +6.7:1 GB	-0.45
Hacker X-30 ESC	-0.4
AeroNaut CAM folder 15X10 + Hub + Spinner	-0.49
Micropilot 2028g + GPS Ant	0.16
Microhard MHX-2400 + Antenna	0.16
UHF control + Antenna	0.16
7.4V 3270mAH Battery	-0.25
7.4V 2000mAH Battery	-0.25
4.8V 250mAh Battery	0

Table 9: Systems Installation Stations – Sunsailor1

9 The Solar Array

As PV cells concept and behavior was never academically taught to anyone on the team, a comprehensive study had to be made. A market review was made in order to find the cells with the highest

Power to Weight Ratio. First, flexible cells were examined. Such cells could be bent over the wing chord and maintain the original airfoil. Unfortunately, highest efficiency that could be found for these cells did not pass 7%. A minimum efficiency that was constrained by the designers was 13%. Finally, a number of thin, fragile cells were examined. The final two candidates were Czech and American products. The Czech cells specific weight is 20% more than the American with 3% less efficiency announced by the manufacturers. However, both cells were too large to be used in one piece and therefore had to be cut to thirds. As availability and cost were also very important the Czech cells were first ordered, as they were more available at the time and were suppose to be received already cut to thirds in a much lower cost than the American cells. However, due to several acquisition problems only a small sample of the quantity was ordered. A ground test for the Czech cells efficiency showed only 13%, while the manufacturer announced 17%. The order was immediately cancelled and the American cells, that meanwhile became available, were ordered. These cells, Sunpower's A-300 cells, are the same ones used for the Helios Solar High Altitude Long Endurance (HALE) UAV. These cells efficiency is over 20% and provided the Sunsailor with sufficient energy even in mid September. The design of the solar array added more constraint on the wing design as it had to carry enough cells for the required voltage and current values. This stage was critical for mold manufacturing as the wing mold was made for the later installation of the solar array over the wing skin. Manufacturing was also a new frontier as very delicate wiring was needed. A visit to IAI MALAM factory was sufficient to understand the basics of work with solar cells. The process itself was documented and later modified for the Sunsailor 2 platform.

Global radiation and winds comprehensive statistical data in the Arava area was contributed by the Israeli Meteorological Service (IMS). The following figure shows the change of radiation in Eilat during the day in every month of the year. All data was taken at ground level.

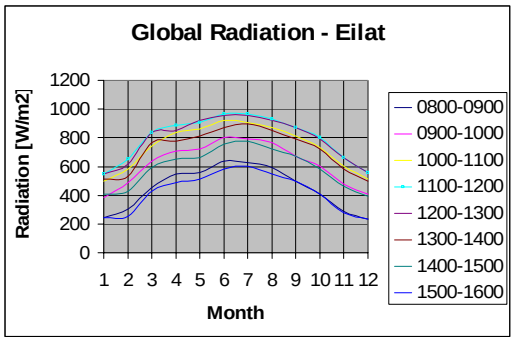

Figure 34: Global Radiation in Eilat.

9.1 Solar Cells Properties

The original A-300 solar cells have a square shape. The following properties are for a third cell after cutting it from the whole and this will be called a cell from now on. Weight includes 0.5 cm wiring to both ends of the cell with the tin soldering. Efficiency is per cell. And maximum performance was measured at 840[W/m^2] Global Radiation. These were measured at the Technion laboratory at the same time of the ground test. All properties are either manufacturer's data or self experiments results (worst case).

Efficiency [%]	20
Open Circuit Voltage [V]	0.67
Short Circuit Current [A]	1.7
Max. Power Voltage [V]	0.59

Max. Power Current [A]	1.2
Temperature Coefficients	
Voltage [mV/°C]	-1.9
Power [%/°C]	0.38
Weight [gr]	3
Dimensions [mm]	125X34
Width [microns]	270±40

Table 10: A-300 Third Cell Properties

9.2 Solar Array Design

Main Consideration for the Solar Array design, once the cells were chosen, was wiring the cells to achieve the required Voltage and Current demands for the motor. The chosen motor work voltage is 11.1V, 14.8V or 18.5V. The chosen driver voltage is a max of 11.1V. Each cell gives about 0.59V at max power (close loop). Connecting the cells in serial gives 0.59V X (Number of cells in Serial) = String Voltage. The current is a factor of the parallel connections. Each string (no matter how many serial cells) gives about 1A in average radiation conditions. 1A X (Number of Strings) = Array's Current. Improvements were made between Sunsailor1 and Sunsailor2 due to the continuous learning process along the project.

For Sunsailor1 we designed an array of 11 parallel strings. Each string had 20 serial cells. The array Output Voltage at maximum power was 11.8V and designed for a max current of 13.2A. Ground tests showed a maximum of 9.8A due to the Mylar layer that covered the cells and produced a smooth airfoil. Another problem was a very unstable Voltage. Every small change of the array angle to the Sun caused great fluctuations in both current and voltage. As voltage became unstable, the speed controller suffered from heating and maximum throttle could not be reached due to a critical drop of voltage when crossing 60% throttle. The following table describes the array tested properties:

Full Array Weight [Kg]	0.75
Max. Power Reached [W]	100
Work Voltage [V]	10.9
Avg. Work Current [A]	7.3
Array Area [m^2]	0.943
Wing Upper Surface Used [%]	70

Table 11: Sunsailor1 Solar Array Results.

This low use of surface was due to the serial wiring. No more 20 serial cells strings could fit in the wing area unless we used the ailerons' surface as well. This was forfeit to avoid electric and mechanic complexity and lower reliability. As a result from this poor performance, the new Sunsailor array was improved.

For Sunsailor2 it was decided to apply three main changes. The use of aileron's surface for solar cells was reevaluated and decided to be simple enough. The array was wired for higher than the necessary Voltage to use more wing area and lesser strings, which means less electric complexity. The third change was forfeiting the Mylar cover and accepting the rough airfoil for a better array efficiency. The array uses 8 parallel strings of 32 cells each. The higher voltage is dropped to a stable 11.4V using a Linear Current Booster (LCB). The LCB also converts the Voltage decrease to Current with 95% efficiency. The only downfall of the LCB is its very high weight. However, the resulted extra power compensate for the additional weight. Also due to a more stable voltage throttle could be used linearly up to 90% (where again voltage drops severely). The new solar array tested properties are described in the following table:

Full Array Weight [Kg]	0.86

LCB Weight [Kg]	0.2
Max. Power Reached [W]	140
Stabilized Work Voltage [V]	11.4
Avg. Work Current [A]	12.28
Array Area [m^2]	1.097
Wing Upper Surface Used [%]	81

Table 12: Sunsailor2 Solar Array Results.

9.3 Solar Array Manufacturing

This was a new frontier for the whole team, as none of the designers ever built such a large and delicate solar array. As already mentioned a tour in IAI MALAM factory gave us the basics for delicate soldering and how to arrange the array itself before wiring and mounting on the wing. A few in-team discussions were made in order to reach the best possible way to mount the ready array to the wing. Many approaches were considered but this article will describe only the selected one. However, mounting was one of the last stages of the solar array manufacturing.

- **PV cells cutting** – as already mentioned the original PV cells had to be cut in thirds to fit to the new paneled airfoil. As laser cut can change the cell composure diamond saw was the best alternative. The sawing doubled the cells price but was mandatory. Prior to that, experiments were conducted to find other ways to bend the cells or cut them. All results led to the saw cutting as the only option. The A-300 cell has three positive/negative connection dots on the back, making it rather easy to later wire every third to the other.
- **Cells Preparation** – each cell has to be cleaned out from both sides, than the electric connection dots has to be covered with Flux, which make the soldering at that point much easier and accurate. Then the cells are placed on a soft mold that fits the wing's upper skin. The cells are held in place using special duct tape.
- **Array Wiring –** going through each string, the cells are connected using a thin silver bar between negative and positive connections. All the strings beginnings and ends wiring are concentrated in the wing's root where they enter an electrical connector that enters the fuselage when the wing is mounted on the fuselage tower.
- **Array Mounting –** finally four small balsa squares are glued to each cell. Then an epoxy resin is used to connect all balsa squares to the wing upper skin, made of thin nylon covering. This reduces inner stresses for the whole array and within each cell. The mounting itself is permanent and done by placing the wing over the array, applying moderate pressure until the epoxy is dry.
- **Array Covering** – Now the array has to be as smooth as possible to improve the flow over the wing. The first Sunsailor used a Mylar covering for that purpose, which caused a 20% loss of array efficiency. The second Sunsailor used transparent duct tape to close the gaps between the cells and the wing skin and between the cells themselves. That solution was less aerodynamic but minimized the efficiency loss to 8%.

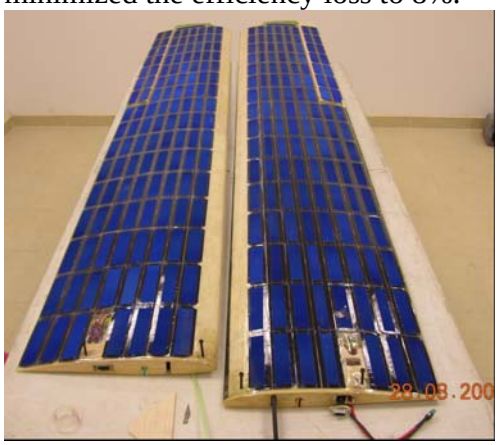

Figure 35: Sunsailor2 Solar Array.

10 Ground Tests

Numerous ground tests were performed before and between the flight tests. The tests were used to confirm structural and performance calculations and to receive comprehensive data for several propellers with the chosen motor.

10.1 Boom Bending NDT

The tail boom was tested for bending. After clamping the larger diameter of the boom, bending forces and moments were applied on the other end. Weight was added up to 50 [N] force with 10 [cm] deflection from the boom center line. Moment was gradually increased up to a rather safe 4[Nm]. Estimation for maximum values was made before the test. Maximum loading was no more than 70% of those estimated to avoid any structural damage. These maximum tested loads were at least 20% higher than those needed during flight according to calculations.

Figure 36: Tail Boom NDT Test.

10.2 Motor and Propeller's Wind Tunnel Test.

As propellers efficiency curves were needed to simulate the propulsion system performance, wind tunnel test was necessary. The Technion Aerospace Engineering Faculty's Wind Tunnel was used .The tunnel walls interference can be corrected according to Pope ea al., but for our low propeller loading, these aren't so big. Also, because of a RPM meter malfunction during the test the results are good for comparison but not for producing accurate Cp Ct curves.
The test system used a Hacker B50-13S Electric motor, Hacker X-30 controller, Lithium Polymer Battery Pack and several different propellers. Along the data recorded were the wind tunnel velocity, propeller RPM, shaft torque, motor current and voltage and propeller output power and thrust. The experiments' data was processed into power and thrust coefficients curves. Using these curves the system's efficiency is easily calculated.
The max efficiencies and work points can be seen for 3 different propellers in the following table.

Diameter X Pitch [inch]	Max. Eff. [%]	Velocity [m/s]	Thrust [N]
13X8	69	11.2	1.75
14X9	62	11.5	3
15X10	65	12	3.2

Table 13: Wind Tunnel Test Results.

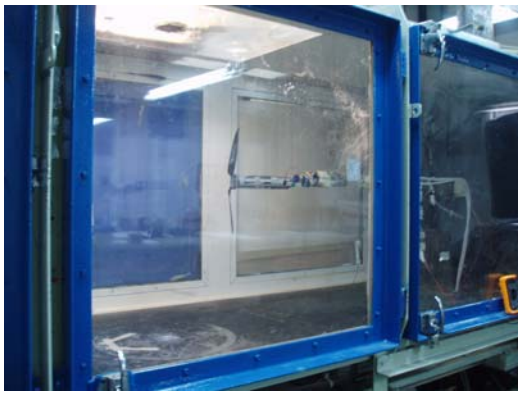

Figure 37: Propeller Wind Tunnel Test

10.3 Wing Bending NDT

The first half wing manufactured lacked shear strength and was used to test the wing under bending. The bending forces were applied as close as possible (with the available means) to the lift distribution along the semi-span. The

wing was loads with a total weight 3.5 times the maximum total lift force for standard flight conditions. Although elasticity of the wing was very large there were no seen plastic effects.

Figure 38: Wing Bending NDT

10.4 Photovoltaic Cells Efficiency Test

Efficiency Tests were taken for both type of cells discussed earlier in this article. Moreover, comparison tests were made for several mounting and covering methods in order to find the most lightweight and high efficiency solution. These two demands always contradict the desire for a more durable array. For both cell types efficiency was checked by measuring the maximum cell power output against the global radiation that was measured at the same spot over the same time interval.
Data was collected for 10 minutes period, every minute. Voltage and Current outputs were measured under resistors' load. Efficiency was later simply calculated by $\eta_{SC} = V \cdot I / Q \cdot A_{SC}$ where η_{SC} is the Solar Cell efficiency, Q is the measured global radiation in Watts and Asc is the Solar Cell radiation collecting Area. The Czech cells were found to have 13% efficiency whereas the A-300 cells were 21% efficiency.

Later, a few mounting and covering methods were tested for power output at same conditions. The following table describes some of the methods and the loss of array efficiency.

Method	Loss [%]
Mylar Cover	10
Transparent Duct Tape - Full	5
Transparent Duct Tape - Borders	1.5
LCB Use	5
MicroGlass Cover	20

Table 14: Loss of array's efficiency for different mounting and and covering methods.

Each method has its own cost in extra weight or less durability and one should choose carefully which method is best for the application at hand.

10.5 Solar Array Manufacturing Tests

As described before a few methods were tested for the array manufacturing. Each method was tested for its durability, flexibility and weight.

Durability – is necessary as the array has to be transported and easily handled on the ground. Therefore, each method was compared to the other by its fragileness when touched, dropped or hit by lightweight work tools (such as those that are used to lock the wing to the fuselage). This was a qualitative.

Flexibility – another qualitative test was comparing the flexibility of the single cell and the whole array for each method. Cell flexibility allows a smoother airfoil while a flexible array is needed to handle the wing aero-elasticity.

Weight – additional weight was checked for every method. Later, each method was examined, trying to lower that

weight, using lighter or less materials. The weight estimations for each method for the Sunsailor2 Solar Array are shown in the following table.

Method	Additional Weight [grams]
Mylar Cover	20
Duct Tape Border Cover	20
Duct Tape Full Cover	150
MicroGlass Sandwich	100
Balsa Spacing	50
Cells Glass Carpet	300

Table 15: Additional Weight for different Solar Array Manufacturing Methods

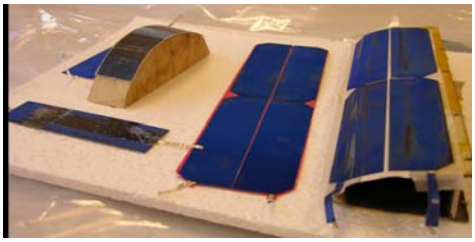

Figure 39: Solar Array Manufacturing Methods

10.6 Solar Array Wind Cooling Test

A fundamental problem of the solar cells is heat. The power degradation due to heat is 0.38% for every 1 degree Celsius over 25 degrees. The average temperature for the record flight season along the flight route is about 32°C which means a loss of 2.66% in array power. The test was conducted in order to simulate and better understand the effect of air flow over the solar array for cooling purposes. A small demonstration array of 20 serial cells was manufactured for the test. The array was connected to resistors to simulate a load. Voltage and current readings were taken every minute for 30 minutes. Temperature values were also taken using a thermocouple bonded to the back of one of the cells in the array. The array was attached to a car's roof to simulate the wing movement through the air. The test began with 5 minutes exposure to the sun, when the array is idle near to the record flight takeoff point. This part of the test was used to confirm the manufacturer data. The array heated up to 60°C causing a loss of 12.5% efficiency, close enough to the manufacturer 13.3%. Then data was logged for 10 minutes in a 30 kilometers per hour (kph) driving speed. 10 minutes driving 40 kph. Finally, 5 minutes driving 50 kph. Every phase the car stopped and the wind velocity was checked. The data was later calibrated accordingly. The results show that air flow cooling is very effective when the array is not covered. It decreases temperature by 20 degrees in less than one minute at 50 kph. However, when covered with Mylar, the cooling effect is much slower and after 5 minutes at 50 kph temperature steadied at 50°C.

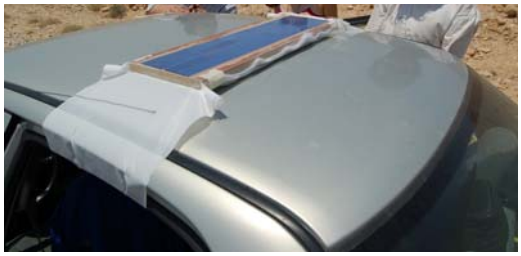

Figure 40: Solar Array Wind Cooling Test.

10.7 Subsystems Power Source Test

Since avionics and servos are using Lithium Polymer (LiPo) batteries for the whole flight, the batteries capacity had to be tested to comply with the estimated endurance. Endurance for the record flight was estimated at less than 3 hours, the batteries were tested for 4 hours at worst case scenario. This means that all

4 servos are working every 3 seconds receiving commands from the autopilot that receives commands from the ground station. The whole system was operated under these conditions for 4 hours and showed that the selected batteries can provide enough power for the record flight.

11 Flight Tests

Sunsailor 1

11.1 Flight Test 1 – Configuration A

Date: 28.4.06
Location: Near Haifa, North Israel.
Duration: 14 minutes
Power Source: LiPo Battery.
Objectives: Checking the platform itself for stable flight and structural integrity.
Description: The maiden flight of Sunsailor1 was performed mainly for safety reasons before installing the autopilot and solar cells.

11.2 Flight Test 2 – Configuration B

Date: 1.6.06
Location: Near Lod.
Duration: 12 minutes
Power Source: LiPo Battery.
Objectives: Downloading telemetry from the autopilot and later calibrating it.
Description: The flight was very stable. The telemetry data was very close to the calculated performance.
(See Appendix A for the Pre-flight checks picture)

11.3 Flight Test 3 – Configuration B

Date: 8.6.06
Location: Near Lod.
Duration: 18 minutes
Power Source: LiPo Battery.
Objectives: Testing autopilot performance.
Description: After a user controlled takeoff the autopilot was given full control over the aircraft. It demonstrated a stable flight, maintaining height and direction vectors and performed an easy point-to-point navigation. Landing was performed with user control.

11.4 Flight Test 4 – Configuration C

Date: 29.6.06
Location: Near Haifa, North Israel.
Duration: 22.5 minutes
Power Source: Solar Array.
Objectives: Demonstrating solar flight and measuring motor heating and power input.
Description: The flight was all radio controlled, performing a slow but stable takeoff and climb. The secondary objective was to measure the motor heating during and after flight and the solar array power output. In order to do this, a thermocouple ring was assembled over the motor case. The readings were logged in a data logger card not connected to the aircraft's telemetry. The data logger was also connected between the solar array and the motor logging the array's output voltage and current. After landing the data was downloaded. It was determined that the motor does not exceed its working temperature of 70°C. It does however show a rise of 11°C right after landing when air-cooling has stopped. The next figure shows a stable 48°C during flight and a rise to 59°C after landing. Even the higher temperature is still in the motor working temperature safe range.

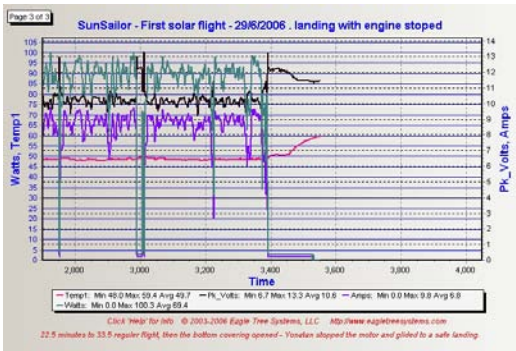

Figure 41: Solar Flight Data Logger Results.

The maximum power output as can be seen is 100[Watts]. Large fluctuations can be witnessed in the array output power due to a constant change of the sun-array angle during flight. Some substantial power decreases also demonstrate the array's high sensitivity to the sunlight angle. These drops mostly occur while the aircraft is in a steep turn (30° and more) against the sun.

11.5 Flight Test 5 – Configuration C
Date: 11.7.06
Location: Near Lod.
Duration: 20 minutes
Power Source: Solar Array.
Objectives: Ensuring structural and electrical integrity before record flight.
Description: Final flight-test with/without autopilot to rehearse control transfers and emergency procedures.
(See Appendix A for the Pre-flight checks picture)

11.6 Record Flight & Crash
Date: 12.7.06
Location: Arava, South Israel.
Duration: 6 minutes
Power Source: Solar Array..
Objectives: Setting a new world record for solar flight.
Description: After takeoff and a very fast climb to 1000 feet, the pilots entered the leading car and began driving from the takeoff area to the main road. In order to maintain eye contact with the aircraft the leading pilot rolled it to the left. Seconds later the plane entered a deep dive and lost structural integrity at 600 feet above ground level. Last velocity reading showed 70 knots.

(See Appendix A for the Sunsailor Team picture)

Sunsailor 2

11.7 Flight Test 1 & Crash
Date: 4.9.06
Location: Near Petah-Tikva.
Duration: 8+38 minutes
Power Source: Solar Array.
Objectives: Aircraft's maiden flight, flying full hour with/without autopilot.
Description: Several minutes after takeoff the pilot noticed a short motor cut-off. Power returned immediately. The cut off was experienced again after another minute and it was decided to land the aircraft at once. The motor and controller were examined and no problems were found. Speed controller cut-off at low voltage was cancelled. Ground tests were performed before the next takeoff making sure the solar array produces enough power for the motor at all flight angles (to the sun – See Appendix A for the Solar Array Ground Check).
After a second takeoff, no problems were encountered for the first 20 minutes. Than the GCS (Ground Control Station) started reporting of low servos voltage every few minutes. As the pilot encountered no problems with the controls the warning was ignored. Autopilot was engaged and performed a stable flight however lost some altitude. At 300 feet the pilot took control and climbed to 500 feet. During climb the pilot lost controls and switched servos power to the back-up battery (Primary

power supply for servos from solar array).
After 500 feet pilot switched back to primary power supply and controls worked properly. Flight test engineer decided to continue the flight. Autopilot received control. After 34 minutes GCS warned for low servos voltage for a few seconds period, much longer than before. Pilot immediately took control and switched to back-up battery. After making sure controls work properly the pilot switched to primary and autopilot control. This switch occurred at 300 feet. Autopilot received command to climb to 500 feet.
During the next period flight was stable but autopilot did not succeed climbing. After 38 minutes the aircraft entered a fast growing down pitch. The pilot identified the problem when the pitch angle was almost vertical. Pilot immediately took controls but did not switch to back-up battery. At 100 feet the pilot succeeded pulling up, but as velocity was too high the plane could not escape the dive and crashed at 45 degrees to the ground.

12 Crashes Investigations

Using the flight data recorder, eyewitnesses and other inspections both crashes were investigated until the reason for the crash was proved beyond any doubt. Conclusions were made and implemented on next applications.

12.1 First Crash Investigation

After a comprehensive investigation, the following conclusions were made:
- After 6 minutes a steep roll to the left cause the V-Tail to break fully or partially.
- As a result of the tail loss the aircraft lost it's longitudinal stability and down pitch angle grew to 90 degrees.
- As a result of the tail loss elevator and rudder controls were obsolete. From black box data it is obvious that the pilot commands were received but tail controls did not react.
- The pilot did succeed to use ailerons seconds before the wing broke down. This also implies on tail loss and not a receiver/autopilot problem.
- Later inquiry of the many witnesses to the crash discovered that one of them saw the tail breaks down first.
    - This last evident concluded the investigation.
    - The tail was built from Balsa and a Mylar skin and was very lightweight. The buckling had probably started at the join of the 2 part of the tail that was the weakest.
    - The next tail was manufactured with much higher strength and carbon reinforcement at the join. The extra weight was balanced by adding the LCB in the front of the fuselage.
    - As reliability of the servos was also questioned during the investigation, they were also replaced.

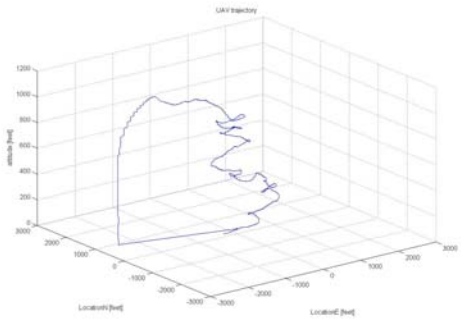

Figure 42: Flight Trajectory – Takeoff to Crash

12.1 Second Crash Investigation

Results and Conclusions were as following:
- Examining the flight data recorder and eyewitnesses it was found that the motor

received full throttle command from the autopilot but motor did not work. Pilot took control with throttle set to idle to reduce loads when pulling up.
- Time from pitch down start to crash was 3 seconds and left the pilot very little time to escape the dive.
- This very small time frame could be avoided by flying at higher altitude. Minimum height for autopilot control was consequently set to 500 feet.
- Since the controller BEC is requires very little power to operate the servos it is impossible that the solar array could not sustain the servos.
- Moreover, the other control losses happened while motor was at full power. When the motor has enough power, the BEC must have enough as well.
- Later consultations with the controller manufacturer, ground test and all the evidences showed that the controller heating was the reason for the controls loss and consequent crash.
- As the chosen controller was very small and had small current limit it heated-up to a temperature where it had to restart itself to prevent and damages.
- When the controller restart, it cuts-off both motor and BEC. These will both return only when throttle is at idle for safety reasons.
- As the autopilot corrects altitude with motor it used full throttle trying to prevent the dive. Velocity is corrected with pitch angle control. However when the BEC cut-off occurred elevator position was on a small down-pitch angle. As this position was constant, pitch grew bigger until reaching a vertical dive. Servos started working only when the controller received idle throttle command from the pilot.
- It was decided to use a much larger and higher current controller for next applications to avoid such heating.
- Better air-cooling is needed for the ESC when flying for long time.
- For less than 6 hours flight it was decided to use a battery for servos operation to increase reliability at the expense of another 200 grams.
- The manual control switch “On” position was towards the pilot (on the transmitter). Back-up battery switch “On” position was to the opposite side. When rapidly taking control the pilot instinct is to pull both switches. Therefore it was decided to invert the back up switch “On/Off” positions.
- Final and most important conclusion was that a servo or motor warning or cut-offs during flight tests compels a quick landing and comprehensive examining until fully understanding and solving the problem.

Appendix A

Pre-Flight Checks

Figure 43: Pre-Flight Checks – Flight Test 2.

Figure 44: Pre-Flight Checks, Power Supply – Flight Test 5

The Sunsailor Team

Figure 45 : The Sunsailor Team

Sunsailor2 Takes Off

Figure 46: Sunsailor2 Takes Off.

Sunsailor2 Landing

Figure 47: Sunsailor2 Landing

Sunsailor2 Solar Array Ground Check

Figure 48: Solar Array Ground Check at different angles.

References

[1] Raymer, D.P., Aircraft Design: A Conceptual Approach, 3rd edition, AIAA Education Series.
[2] Etkin, B. and Reid, L.D., Dynamics of Flight (Stability and Control), John Wiley & Sons, Inc, 1996
[3] Perkins, C.D. and Hage, R.E., Airplane Performance, Stability and Control, John Wiley & Sons, 1949
[4] AVL software by Mark Drela & Harold Youngren.